Dmitrenko, I.A.; Kirillov, S.A.; Rysgaard, S.; Barber, D.G.; Babb, D.G.; Pedersen, L.T.; Koldunov, N.V.; Boone, W.; Crabeck, O.; Mortensen, J.:

Polynya impacts on water properties in a Northeast Greenland fjord

In: Estuarine, Coastal and Shelf Science (2014) Elsevier

DOI: 10.1016/j.ecss.2014.11.027

Polynya impacts on water properties in a Northeast Greenland Fiord

Igor A. Dmitrenko[1*], Sergey A. Kirillov[1], Søren Rysgaard[1,2,3], David G. Barber[1], David G. Babb[1], Leif Toudal Pedersen[4], Nikolay V. Koldunov[5,6], Wieter Boone[1], Odile Crabeck[1] and John Mortensen[2]

[1]Centre for Earth Observation Science, University of Manitoba, Winnipeg, Canada

[2]Greenland Climate Research Centre, Greenland Institute of Natural Resources, Nuuk, Greenland

[3]Arctic Research Centre, Aarhus University, Århus, Denmark

[4]Danish Meteorological Institute (DMI), Copenhagen, Denmark

[5]Institute of Oceanography, University of Hamburg, Germany

[6]now at Climate Service Center 2.0, HZG, Hamburg, Germany

*Corresponding author, e-mail: igor.dmitrenko@umanitoba.ca

Abstract: Polynyas are an important yet poorly understood phenomena of high latitude oceans. A storm event during late December 2013 with down-fjord winds of up to 25 m/s forced the collapse of the landfast ice over the Young Sound (YS) fjord outlet in northeast Greenland. This storm created a coastal polynya that was further maintained by several consecutive wind events until early March 2014. During the polynya period, three landfast ice-tethered oceanographic moorings recorded an enhanced surface layer (~0-40 m) transport towards the mouth of YS and a layer below (~40-140 m) flowing into the fjord and supplying the interior with cool and saline water from the polynya. Subsequent CTD transects in May 2014 reveal that this lower layer contained polynya originated cool, saline and oxygen enriched water with oxygen concentrations significantly exceeding values from the previous summer. Salt balance bulk estimates show that the polynya generated a sufficient amount of brine to ventilate the fjord interior.

Keywords: Fjord dynamics; Polynyas; Fast ice; Mooring systems; CTD observations

Introduction

Young Sound (YS) is located in Northeast Greenland at ~74°N and represents a relatively deep (340 m) and long (~90 km) high latitude fjord with a 40 m deep sill at the mouth (Figures 1a and 1b). YS is covered by landfast ice from late October to the beginning of July [*Bendtsen et al*., 2014]. During winter, the landfast ice cover extends 10-30 km from the fjord mouth, thereby eliminating wind stress on the water column. Further offshore in the transition zone between the landfast ice and pack ice, one of the

most prominent polynyas in northeast Greenland is maintained during winter by sustained northerly winds [*Pedersen et al*., 2010].

Openings in the sea ice cover, i.e. polynyas, allow for intense thermodynamic sea ice formation and brine release causing dense water formation [*Rudels,* 1990]. Polynyas occur over continental shelves around the Arctic Ocean [*Winsor and Bjoerk,* 2000; *Tamura and Ohsima,* 2011] and are generally created and maintained by latent and/or sensible heat processes [e.g., *Barber and Massom,* 2007]. Over these shallow continental shelves it is generally expected that during winter the oceanic heat flux to the landfast ice is small because the entire water column is close to the freezing temperature. Brine rejection associated with ice formation results in brine-enriched shelf waters, which help maintain the cold upper halocline in the Arctic Ocean [*Aagaard et al., 1981*]. Dense shelf waters accumulating near the bottom have been shown to occur in Storfjorden, Svalbard [*Anderson et al.,* 2004; *Fer et al.,* 2004], on the northwestern shelf of the Okhotsk Sea [*Shcherbina et al.,* 2004] and along the Russian Arctic shelf [*Dmitrenko et al,* 2005; *Bauch et al*., 2012].

Arctic polynyas produce dense water during thermodynamic ice growth, thereby affecting the renewal and ventilation of the deep water in Arctic fjords [e.g., *Skogseth et al*., 2013]. However the associated water dynamics remain poorly understood due to scarcity of in situ observation, specifically along the East Greenland Shelf. In fact, very little information is available on the oceanographic conditions in coastal areas and the numerous deep fjords of Northeast Greenland. Research and monitoring carried out at the Zackenberg/Daneborg research stations (Figure 1b, *Rysgaard and Glud*, 2007) therefore provide the only long-term records for characterizing fjord dynamics and near-coastal

water masses along the northeast coast of Greenland. Here we report on oceanographic observations at three landfast ice-tethered moorings (October 2013 – May 2014) and along-fjord transects (May 2014) in YS. From December 2013 to March 2014, a coastal polynya was maintained adjacent to the YS mouth by down-fjord wind events during which wind speeds reached 25 m/s. The polynya-induced brine production enhanced water circulation replenishing the fjord's intermediate (40-140 m) layer with polynya generated water.

Data and methods

Between October 2013 and May 2014, four landfast ice-tethered moorings were deployed from the stationary landfast ice in YS (Figures 1b and 1e). The YS13-m01/m02/m03/m04 moorings were anchored at locations with water depths of 58/82/158/340 m, respectively. All moorings carried a combination of 300 kHz downward-looking Workhorse Sentinel acoustic Doppler current profilers (ADCPs) by Teledyne RD Instruments, and Sea-Bird Electronics, Inc., SBE-37s with conductivity-temperature-depth (CTD) sensors (moorings YS13-m01/m03) or McLane mooring profilers (MMPs) with SBE 52-MP CTD sensor (moorings YS13-m02/m04). About one month after deployment, both MMPs failed for regular profiling along a mooring line and stopped near the bottom, but still collected data until recovery in May 2014. For this research we use only the MMP CTD time series from m02 at 80 m. On mooring YS13-m03, seven SBE-37s recorded conductivity and temperature at discrete depths every 10 minutes. For this study, we use data from the SBE-37 deployed at 77 m. Mooring YS13-m01 was lost when the landfast ice broke up over the YS mouth in December 2013

(Figure 1d and 1e). The velocity data from the ADCPs were taken at 2 m depth intervals, with a 10-minute ensemble time interval and 20 pings per ensemble. The first/last bins were located at 6/84 m except m02 where the last valid bin was at 78 m.

Mooring-based observations were complemented by four along-fjord CTD transects taken between 4 and 28 May 2014 with an SBE-19plus CTD equipped with a dissolved oxygen (DO) sensor SBE-43. The CTD transects show insignificant temporal variability. CTD transects from May 2014 are supplemented by profiles collated during mooring deployment in October 2013 and an along fjord CTD transect from August 2013 during the ice free summer.

According to the manufacturers' estimates, individual temperature and conductivity measurements are accurate to ±0.005°C and ±0.0005S/m, respectively, for the SBE-19plus, to ±0.002°C and ±0.0003S/m, respectively, for the SBE-37s and SBE 52-MP. The accuracy of DO sensor is ±2% of saturation. For thermohaline conditions in the YS intermediate water layer (40-140 m) it corresponds to ~±0.18 ml/l. The ADCP velocity precision and resolution are ±0.5% and ±0.1cm/s, respectively. The ADCP velocity estimated error is 1.55cm/s. Compass accuracy is ±2.7° and was corrected by adding magnetic deviation (-18.5°). The ADCP internal temperature sensor is not calibrated and used only for reference. The CTDs were calibrated before the expeditions.

Ice conditions over the YS mouth were monitored by 23 advanced synthetic aperture radar (SAR) images acquired between November 2013 and April 2014. SAR satellite-mounted instruments transmit radar signals and then measure how strongly those signals are scattered back. In general, the newly formed sea-ice, polynya open water, frazil ice, and landfast ice edge are distinguishable in SAR imagery (Figure 1c-1d). Three polynya

regions are defined around the YS mouth and are delineated by yellow dashed lines in Figure 1e. Sea-ice concentration data from these regions at three pixels (p1, p2 and p3 in Figure 1e) of the Advanced Microwave Scanning Radiometer 2 (AMSR2, successor of AMSR-E; 3.125km resolution) are used to quantify the size of the coastal polynya over the YS mouth (for more details on AMSR2, sea-ice concentration algorithm and AMSR2 ability to resolve the flaw lead open water see *Beitsch et al*., 2014). Visually comparing AMSR2 to various other satellite images (http://ocean.dmi.dk/arctic/daneborg.uk.php) we note a strong level of agreement between the different platforms. Except for during April and May 2014 when AMSR2 artificially observed episodic reductions in sea ice concentration (Figure 2a) that are not verified by other satellites.

Hourly observations of surface air temperature, wind velocity and direction were retrieved from the Daneborg automated meteorological station maintained by DMI (location in Figure 1b). Wind data shows that 83% of storm events in which wind velocity exceeded 10 m/s came from the north with northerly winds (0±30°). During the CTD transects of May 2014 sea-ice thickness was measured at all stations.

Results

A storm event on 18-25 December 2013 with northerly winds (348±15°) with a mean velocity of 15.3±4.4 m/s and maximum velocity of 25.2 m/s forced the collapse of the landfast ice over the YS outlet to the Greenland Sea on 20 December (Figures 1c, 1d, 2a, and 2b). By 26 December, the piece of broken off fast-ice had been transported ~30 km downwind from the mouth of YS (Figure 1d). Consequently, the landfast ice edge stabilized 20 km further into the fjord, or roughly 3.5 km behind the entrance sill and

~400 m from the mooring YS13-m02 (Figure 1e). The December storm created a coastal polynya that was maintained until early March 2014 by several consecutive strong northerly wind events exceeding 15 m/s (Figures 2a and 2b). After 4 March, landfast ice thermodynamically grew within the polynya area and remained intact until the ice cover broke up on 17 June 2014 (not shown).

Following the polynya opening, mooring YS13-m02 recorded a drop in water temperature of ~0.15°C and 0.12 increase in salinity at 80 m depth (Figures 2c and 2d). Mooring YS13-m03 (5.14 away, Figure 1e) shows a similar tendency at 77 m depth. During the polynya period, which lasted from 20 December 2013 to 4 March 2014, moorings m02/m03 at 80/77 m depth show salinity gradually increased by ~0.5, and temperature decreased by ~0.16°C (Figures 2c and 2d). In fact, every single wind event exceeding 10 m/s was accompanied by a salinity increase with the magnitude likely linked to wind speed, fraction of open water and air temperature. For example, after the polynya formed the first strong wind event in 5-12 January with wind speed up to 15 m/s (Figure 2b) acted in combination with low sea ice concentrations (Figure 2a) and air temperatures below -10°C (Figure 2b) caused the peak salinity increase of 0.27 to occur at both m02 and m03 (Figure 2c). The m02 temperature at 80 m showed potential supercooling (i.e. temperature is below the freezing temperature in reference to the surface) of up to -0.014°C at the end of the first and second wind events (Figure 2d), which coincided with maximum polynya openings (Figure 2a). This range of supercooling is similar to that reported for the Arctic polynyas by *Skogseth et al.* [2009] and *Dmitrenko et al*. [2010b]. In contrast to 77-80 m, the surface layer (2 m depth) tended to be warmer by up to 0.3°C during the period between 25 December, 5 days after the

polynya opened, to 4 March, when the polynya closed (moorings m02 and m03, Figure 2e). Mooring m04 shows a similar tendency though the signal is much weaker given the distance from m04 to the polynya.

The time series of both temperature and salinity at moorings m02 and m03 (separated by 5.1 km; Figure 1e) shows contrary lagging tendency at the surface and 77-80 m, indicating reverse water flow between the surface layer and the layer below. For the polynya period, the time-lagged correlation between the m02 and m03 salinity and temperature time series in the lower layer shows that salinity and temperature at m02 advanced those at m03 by 2.12 days (Figures 2c and 2d) suggesting water flowed into YS at depth with a mean velocity of 2.8 cm/s. For the surface layer, temperature at m02 lagged that at m03 by 1.16 days (Figure 2e) revealing a mean outflow velocity of 5.1 cm/s.

These estimates are in agreement with velocity observations at all 3 moorings clearly showing reverse water flow and enhanced velocities during polynya opening (Figure 3a). During the polynya period, the surface ADCP bin at m02 and m03 showed mean outflow velocity of 6.1±2.9 cm/s and 5.3±2.6 cm/s, respectively, vs. 5.1 cm/s estimated from the above lagging analysis. The deepest ADCP bin showed mean inflow velocity of 1.6±1.35 cm/s and 2.6±1.7 cm/s vs. 2.8 cm/s based on the lagging procedure (Figure 3). Overall, during the polynya period the velocity in the upper 80 m of the water column is characterized by a two-layer structure with an outflow in the 40 m thick surface layer and an inflow in the layer below (40-80 m). At all three moorings, the average outflow velocity over the whole 40 m thick surface layer was ~2-4 cm/s which was two times

greater than the average inflow velocity in the deeper layer (40-80 m) of ~1-2 cm/s (Figures 3d and 4a).

The CTD vertical profiles from May 2014 identify the depth of the winter-modified lower layer to be located between 40 and 140 m (Figure 4). They also provide evidence for an advective origin of this layer. The CTD profiles taken at YS13-m04 in October 2013 and May 2014 show seasonal cooling and salinization down to 150 m delineating the depth of the seasonal signal penetration (Figure 4b). From the top, however, this layer is delineated by the intermediate temperature maximum between 30 and 40 m depth indicating the actual depth of winter vertical mixing associated with sea-ice formation. Thus, winter vertical mixing fails to explain the fall-to-spring water column modification in the 40-140 m layer. The subsurface warm layer represents the remnant of summer heating preserved below the halocline and extends from the fjord interior to outer fjord gradually cooling from -1.7°C over the interior sill to -1.74°C at m03 (Figure 4c). The outward flow of this subsurface warm layer is also recorded during polynya opening (Figures 2e and 3a). The underlying water in 40-140 m is weakly stratified (salinity 32.25-32.35) and almost homogenous with temperature (-1.75 to -1.76°C) slightly exceeding the potential freezing temperature by 0.008-0.018°C. Furthermore, it is supersaturated with oxygen (106-107%, not shown) at concentrations 9-9.2 ml/l (Figures 4b and 4e) significantly exceeding the August concentrations 6.25-7.25 ml/l (not shown). The anomalous vertical distribution of all parameters at station 69 (Figure 4c-4e) is poorly understood and likely to be a local pattern determined by fjord configuration.

The advective origin of the layer between 40 m and 140 m is also evident from the salt balance between fall and spring. The October-to-May seasonal salinization at YS13-

m04 (Figure 4d) would require the formation of a fast ice cover 4.6 m thick with a bulk salinity of 6 (*Ryan Galley, pers. comm.*) using the approach suggested in [*Dmitrenko et al*., 2009]. However, the ice thickness was only 1.1 m, hence the extra salt required had to be laterally advected in accordance to our velocity observations (Figure 3). The salt balance calculations for YS13-m02/m03 gave similar regularity.

Discussion

The data from both moorings and hydrographic surveys corroborate the polynya origin of the layer between 40 and 140 m in the interior of YS. Thermodynamic ice formation under cold air temperatures down to -30°C (Figure 2b) combined with continuous removal of ice by northerly winds makes the polynya area very efficient in providing salt input to the underlying water. The brine release associated with polynya frazil ice formation in supercooled water modifies surface water into cool and brine-enriched saline water observed at m02 and m03. The oxygen rejected from the frazil ice to the water column results in oxygen supersaturation in the polynya generated-water [*Glud et al*., 2002]. On the fjord-side of the sill, the gravity current of dense, brine-enriched water supplies the interior of the fjord with cold, saline and oxygen enriched water as recorded by our moorings and observed during our CTD surveys (Figures 3 and 4).

The entrance sill creates a topographic barrier between the fjord and adjacent shelf area. The fjord-shelf exchange during winter 2013-2014 is unresolved with oceanographic observations and therefore poorly understood. In the following, however,

we speculate on the role of polynya-modified shelf water in generating the YS intermediate layer.

The cross-shelf exchange with the warm Atlantic water boundary current may occur in response to wind forcing resulting in an extensive spreading over the shelf and adjoining high-Arctic fjords of Atlantic water or Atlantic-modified shelf water [e.g., *Cottier et al*., 2007; *Dmitrenko et al*., 2010a]. In Northeast Greenland, the Atlantic water is supplied by the East Greenland Current. This Atlantic water is derived from the West Spitsbergen Current that sets northward along the west coast of Spitsbergen and water from the Atlantic layer of the Arctic Ocean [e.g., *Aagaard and Coachman*, 1968; *Mauritzen*, 1996]. The relatively warm (0-2 °C) Atlantic water resides at ~150-800 m depth forming a layer below the Polar water [*Rudels et al*., 2002].

The YS13-m02 bottom temperature time series shows that events of potential supercooling alternate with relatively warm events during which temperature exceeds potential temperature of freezing by 0.03-0.08°C (Figure 2d). This suggests episodic inflow of relatively warm and saline shelf water above the entrance sill. The down-fjord wind creates open water over the YS mouth and favors upwelling on the shelf-side of the sill. While the true warm Atlantic water with positive temperatures is not observed over the YS mouth, at st. 44 (~3.5 km off the sill, Figure 1b), the intermediate layer is modified by interaction with Atlantic water and temperature starts to increase with depth only 20m below the sill at a depth of 60m (Figure 5a). The wind-driven upwelling of this saltier and relatively warmer water up to the sill depth combined with cross-sill tidal flow can transport slightly warm and saline water into YS, generating episodic “warm conditions” following down-fjord wind events (Figure 2d). However, oxygen

supersaturation in the YS intermediate layer clearly identifies brine from ice growth within the polynya as its primary source.

The polynya-modified shelf water at the shelf-side of the sill is likely to be an important source for the YS water between 40 and 140 m. To investigate this further, we focus on the capacity of the fjord and shelf polynya (polynya region 1 and regions 2+3, respectively, in Figure 1e) in ventilating the fjord interior by generating the saltier water recorded in YS in May 2014 (Figures 4b and 4d). More specifically, we link the seasonal salinity adjustment to winter ice formation following the approach used by *Dmitrenko et al*. [2009].

The difference in salt content within YS between October 2013 and May 2014 is considered to be a measure of the salinity field adjustment to winter sea-ice formation assuming there is only salt water influx to YS over the entrance sill for compensating the sea-ice outflow from the polynya. At the moment there are no available data to justify this assumption and/or estimate the error associated with this assumption. Another assumption is that ice formed in the polynya is only the frazil ice continuously removed from YS by wind.

In the following, we focus on evaluating the polynya sea-ice production from October 2013 to May 2014 (h_{ip}) suggesting the balance between the YS salt content in May and October. Equation (1) assumes balance between (left) the water and sea-ice salt content in May (first and second terms, respectively) and (right) the initial salt content in October (third term), the salt removed from YS with polynya-generated frazil ice (fourth term) and injected to YS with shelf water entering the fjord above the sill for compensating the removal of frazil ice (last term):

$$\int_0^{H-h_{if}} S_2(z)A(z)\rho_w(z)dz + S_{if}h_{if}A(0)\rho_{if} = \int_0^{H} S_1(z)A(z)\rho_w(z)dz - S_{ip}h_{ip}a\rho_{ip} + S'h_{ip}a\rho'_w \quad (1),$$

where $S_1(z)/S_2(z)$ are water salinities in October/May, H is the lower depth of seasonal salinity changes (150 m, Figure 4b), $\rho_w(z)$ - water density, S' (32.3, Figure 4d) and ρ'_w (1026.1 kg/m^3) are the bottom water salinity and density at the sill, respectively, $A(z)$ is partial area of fjord interior, a – polynya area. The fjord polynya 1 (a=11.75 km^2, Figure 1e) is about 3.8% of the fjord area limited by the entrance sill from one side and cut off at the position of mooring YS13-m04 ($A(0)$=238.2 km^2). This cut-off is based on the assumption that the polynya generated water penetrates into the fjord interior only to YS13-m04 that follows from the along-fjord temperature and DO distribution in Figures 4c and 4e. h_{if}, S_{if}, ρ_{if} are the mean landfast ice thickness, salinity, and density measured in May 2014: 1.10 m, 6 [*Ryan Galley, pers.comm*] and 900 kg/m^3, respectively. The unknown polynya-generated cumulative frazil ice thickness h_{ip}, computed from (1) for density ρ_{ip}= 950 kg/m^3 [*Martin and Kauffman,* 1981] and salinity S_{ip}=0.31·$S_2(z=0)$ [*Winsor and Bjoerk*; 2000], is estimated at 93.5 m or 1.10 km^3.

The sensitivity study reveals no significant variation of h_{ip} in response to uncertainties associated with accuracy of parameters used in (1). For example, the landfast ice density (ρ_{if}) changing ±10 kg/m^3 results in ±0.4 m of cumulative ice production in the polynya. The uncertainty in ice thickness h_{if} =±0.06 m, taken as a standard error of the mean for the ice thickness measurements in May, and ice salinity of ±10% impact the ice production by ±1.8 m and ±0.5 m, respectively. The alteration of bottom water salinity at the sill from 32.3 (Figure 4d) to 31.8 (as measured in August 2013, not shown) results in

1.9 m decrease of cumulative ice production. The most significant change of h_{ip} is associated with uncertainty in S_{ip}. The S_{ip} variation ±10% causes the ice production to differ ±3.9 m. The implication of salinity data from August 2013 (not shown) for estimating the third term in equation (1) results in additional 6.4 m frazil ice (99.9 vs 93.6 m). Extending the fjord area to the interior sill ($A(0)$=308.4km^2) yields 1.29 times greater ice production.

The mean winter cumulative sea-ice production in the Arctic coastal polynyas is estimated to be up to 19 m [*Tamura and Ohshima*, 2011]. For the coastal polynya in Storfjorden (Spitsbergen), for winters 1998-2002, *Skogseth et al*. [2013] estimated the accumulated frazil ice thickness to be 13.1-19.5 m. For the 23-day polynya event in February–March 2004 in the Laptev Sea, *Krumpen et al.* [2011] estimated the frazil ice growth to be 8 m. For the 9-day polynya event in February-March 1993 near Banks Island (Canadian Archipelago), *Winsor and Bjoerk* [2000] estimated the accumulated ice growth to be 1.2 m with a maximum ice growth rate of 0.27 m/day. We take this value as an upper bound for the ice growth rate within a polynya. Following this estimate, for the 73-day polynya event in YS (Figure 2a) we may expect O(h_{ip})~20 m. This is significantly less compared to h_{ip}=93.5 m estimated from equation (1), indicating that polynya region 1 alone is not capable for maintaining the salt balance prescribed in (1). Extending the polynya area to polynya regions 1+2 (11.75+26.88 km^2, Figure 1e) yields h_{ip}=28.5 m that still exceeds a realistic value. Only the combination of polynya regions 1, 2 and 3 (11.75+26.88+55.81 km^2, Figure 1e) reveals h_{ip}=11.6 m that seems to be reasonable ice production per unit area. Overall, these estimates strongly support the role of polynya-modified shelf water for supplying the YS intermediate layer.

The salinity of the polynya-modified shelf water S=32.25-32.35 is less than the salinity of the YS water below 160 m (S>32.5) – Figures 4b and 4d. This indicates that the polynya alone is unable to ventilate the bottom water of YS at S>33 rising the question on the origin of the YS bottom water. The cross-sill salinity over the mouth of YS at 100 m depth shows the shelf-side salinity 33.1, exceeding that at the fjord-side by ~1 (Figure 5b). We speculate that the upwelling of the saltier water over the shelf-side of the entrance sill accompanied by the cross-sill transport to the fjord by tidal currents contributes to the formation of the YS deep water with salinities exceeding 32.5.

Summary

High latitude fjords lack circulation and corresponding water flushing during winter due to the sea-ice cover limiting wind stress to the water column. Wind-driven circulation is only reinforced when the ice cover breaks up, allowing both dynamic and themohaline processes to dominate ocean-atmosphere exchange [e.g., *Cottier et al*., 2010]. For the silled fjords, inflow from the shelf is impeded by the entrance sill which represents a topographic barrier that slows the replenishment of a fjord's intermediate and deep layers with more oxygenated water. In extreme cases, this may lead to depletion of oxygen [e.g., *Farmer and Freeland,* 1983] resulting in serious consequences for biological activity. In this study, however, we show that the polynya, created by wind forcing over the mouth of YS in December 2013 – March 2014, facilitates water circulation in the landfast ice-covered fjord, even with the presence of a continuous ice cover over the inner fjord, thereby supplying the fjord interior with cool, saline, oxygenated water. Thus, we provide the first evidence of a strong polynya-generated impact of water properties within a high

Arctic fjord in Northeast Greenland. This expands the current view of Atlantic-dominated exchanges observed elsewhere in Greenland [e.g., *Straneo and Heimbach*, 2013].

During winter 2013-14 the gravity current of dense and brine-enriched polynya-modified water enhanced the inflow of water between 40 and 140 m to the interior of the fjord with a corresponding outflow in the surface layer (~0-40 m). Mean velocities within the surface layer were 2-4 cm/s while velocities within the lower layer were 1-2 cm/s. This is evident from both (i) ADCP velocity observations at three landfast ice-tethered oceanographic moorings and (ii) lagging observed in the time series of salinity and temperature at two outer-fjord moorings separated by 5.14 km. The CTD data taken in May 2014 show that the intermediate layer in the outer and mid-fjord were filled with cool, saline and oxygen enriched polynya water. Our bulk estimates show that the circulation cell over the fjord-side of the entrance sill was not closed and inflow of polynya-modified coastal water to YS over the sill was required to explain the fall-to-winter salinity increase in YS. In summary, our data show the role of a coastal polynya in ventilating the fjords interior down to ~140 m while not deep enough to replace the bottom water.

Acknowledgments: This study was funded by the Canada Excellence Research Chair (CERC) program, the Canada Research Chair (CRC) program, the Canada Foundation of Innovation (CFI), the National Sciences and Engineering Research Council of Canada (NSERC, grant RGPIN-2014-03606), the Manitoba Research and Innovation Fund, and the University of Manitoba, Aarhus University and the Greenland Institute of Natural Resources. We thank Ivali Lennert, Kunuk Lennert and Egon Frandsen for outstanding

technical assistance in the field. This work is a contribution to the Arctic Science Partnership (ASP) and the ArcticNet Networks of Centres of Excellence programs.

Reference

Aagaard, K., and L.K. Coachman (1968), The East Greenland Current north of Denmark Strait, Part I, *Arctic*, 21, 181-200

Aagaard, K., L. K. Coachman, and E. Carmack (1981), On the halocline of the Arctic Ocean, *Deep Sea Res*. Part A, 28(6), 529-545, doi: 10.1016/0198-0149(81)90115-1.

Anderson, L. G., E. Falck, E. P. Jones, S. Jutterström, and J. H. Swift (2004), Enhanced uptake of atmospheric CO_2 during freezing of seawater: A field study in Storfjorden, Svalbard, *J. Geophys. Res*., 109, C06004, doi:10.1029/2003JC002120.

Bauch, D., J. A. Hölemann, I. A. Dmitrenko, M. A. Janout, A. Nikulina, S. A. Kirillov, T. Krumpen, H. Kassens, and L. Timokhov (2012), Impact of Siberian coastal polynyas on shelf-derived Arctic Ocean halocline waters, *J. Geophys. Res*., 117, C00G12, doi:10.1029/2011JC007282.

Barber, D. G., and R. A. Massom (2007),,The role of sea ice in Arctic and Antarctic Polynyas, in: *Polynyas: Windows to the World*, edited by Smith, W.O., and D.G. Barber, 74, 1-54, *Elsevier Oceanography Series*, doi:10.1016/S0422-9894(06)74001-6.

Beitsch, A., L. Kaleschke, and S. Kern (2014), Investigating High-Resolution AMSR2 Sea Ice Concentrations during the February 2013 Fracture Event in the Beaufort Sea, *Remote Sens. 6*(5), 3841-3856; doi:10.3390/rs6053841.

Bendtsen, J., J. Mortensen and S. Rysgaard (2014), Seasonal surface layer dynamics and sensitivity to runoff in a high Arctic fjord (Young Sound/Tyrolerfjord, 74°N), *J. Geophys. Res*., doi: 10.1002/2014JC010077.

Cottier, F. R., F. Nilsen, M.E. Inall, S. Gerland, V. Tverberg, and H. Svendsen (2007), Wintertime warming of an Arctic shelf in response to large-scale atmospheric circulation, *Geophys. Res. Lett*., 34, L10607, doi:10.1029/2007GL029948.

Cottier, F. R., F. Nilsen, R. Skogseth, V. Tverberg, J. Skarthhamar, and H. Svendsen (2010), Arctic fjords: a review of the oceanographic environment and dominant physical processes, Geological Society, London, Special Publications, 344(1), 51-60, doi: 10.1144/SP344.54.

Dmitrenko, I., K. Tyshko, S. Kirillov, J. Hölemann, H. Eicken, and H. Kassens (2005), Impact of flaw polynyas on the hydrography of the Laptev Sea, *Global and Planetary Change*, 48, 9-27, doi: 10.1016/j.gloplacha.2004.12.016

Dmitrenko, I. A., S. A. Kirillov, L. B. Tremblay, D. Bauch, and S. Willmes (2009), Sea-ice production over the Laptev Sea shelf inferred from historical summer-to-winter hydrographic observations of 1960s–1990s, *Geophys. Res. Lett*., 36, L13605, doi: 10.1029/2009GL038775.

Dmitrenko, I. A., S. A. Kirillov, L. B.Tremblay, D. Bauch, J. A. Hölemann, T. Krumpen, H. Kassens, C. Wegner, G. Heinemann, and D. Schröder (2010a), Impact of the Arctic Ocean Atlantic water layer on Siberian shelf hydrography, *J. Geophys. Res*., 115(C8), C08010, doi: 10.1029/2009JC006020.

Dmitrenko, I. A., C. Wegner, H. Kassens, S. A. Kirillov, T. Krumpen, G. Heinemann, A. Helbig, D. Schröder, J. A. Hölemann, T. Klagge, K. Tyshko, and T. Busche (2010b),

Observations of supercooling and frazil ice formation in the Laptev Sea coastal polynya, *J. Geophys. Res*., 115, C05015, doi:10.1029/2009JC005798.

Farmer, D. M. and H. J. Freeland (1983), The physical oceanography of fjords, *Progress in Oceanography*, 12, 147-220.

Fer, I., R. Skogseth, and P. M. Haugan (2004), Mixing of the Storfjorden overflow (Svalbard Archipelago) inferred from density overturns, *J. Geophys. Res*., 109, C01005, doi:10.1029/2003JC001968.

Fofonoff, P., and R. C. Millard Jr. (1983), Algorithms for computation of fundamental properties of seawater, UNESCO Tech. Pap. Mar. Sci., 44, 53 pp.

Glud, R. N., S. Rysgaard, and M. Kühl1 (2002), A laboratory study on O_2 dynamics and photosynthesis in ice algal communities: quantification by microsensors, O_2 exchange rates, ^{14}C incubations and a PAM fluorometer, *Aquatic Microbial Ecology*, 25, 301-311.

Krumpen, T., J. A. Hölemann, S. Willmes, M. A. Morales Maqueda, T. Busche, I. A. Dmitrenko, R. Gerdes, C. Haas, G. Heinemann, S. Hendricks, H. Kassens, L. Rabenstein, and D. Schröder (2011), Sea ice production and water mass modification in the eastern Laptev Sea, *J. Geophys. Res*., 116, C05014, doi:10.1029/2010JC006545.

Martin, S., and P. Kauffman (1981), A field and laboratory study of wave dumping by grease ice, *J. Glaciol*., 27, 283–313.

Mauritzen, C. (1996), Production of dense overflow waters feeding the North Atlantic across the Greenland Sea - Scotland Ridge. Part 1: Evidence for a revised circulation scheme, *Deep-Sea Research*, 43, 769–806.

Pedersen, J. B. T., L. H. Kaufmann, A. Kroon and B. H. Jakobsen (2010), The Northeast Greenland Sirius Water Polynya dynamics and variability inferred from satellite imagery, *Danish J. Geography*, 110(2), 131-142.

Rudels, B. (1990), Haline convection in the Greenland Sea, *Deep Sea Res*., Part A, 37(9), 1491–1511, doi:10.1016/0198-0149(90)90139-M.

Rudels, B., E. Fahrbach, J. Meincke, G. Budeus, and P. Eriksson (2002), The East Greenland Current and its contribution to the Denmark Strait overflow, *ICES Journal of Marine Science*, 59, 1133–1154.

Rysgaard, S., and R. N. Glud (2007), Carbon Cycling in Arctic Marine Ecosystems. Case Study Young Sound, *Meddelelser Greenl., Bioscience*, 58, The Comm. for Sci. Res. in Greenl., Copenhagen, 214 pp.

Rysgaard, S., T. Vang, M. Stjernholm, B. Rasmussen, A. Windelin, and S. Kiilsholm (2003), Physical conditions, carbon transport and climate change impacts in a NE Greenland fjord, *Arct. Antarct. Alp. Res.*, 35, 301–312.

Shcherbina, A. Y., L. D. Talley, and D. L. Rudnick (2004), Dense water formation on the northwestern shelf of the Okhotsk Sea: 2. Quantifying the transports, *J. Geophys. Res*., 109, C09S09, doi:10.1029/2003JC002197.

Skogseth, R., F. Nilsen, and L. H. Smedsrud (2009), Supercooled water in an Arctic polynya: Observations and modeling, *J. Glaciol*., 55(189), 43–52, doi:10.3189/002214309788608840.

Skogseth, R., I. Fer, and P. M. Haugan (2013), Dense-water production and overflow from an Arctic coastal polynya in Storfjorden, in: The Nordic Seas: An Integrated

Perspective (eds. H. Drange, T. Dokken, T. Furevik, R. Gerdes and W. Berger), American Geophysical Union, Washington, D. C.. doi: 10.1029/158GM07.

Straneo, F., and P. Heimbach (2013), North Atlantic warming and the retreat of Greenland's outlet glaciers, *Nature*, *504*, 36-43.

Tamura, T., and K. I. Ohshima (2011), Mapping of sea ice production in the Arctic coastal polynyas, *J. Geophys. Res*., 116, C07030, doi:10.1029/2010JC006586.

Winsor, P., and G. Bjoerk (2000), Polynya activity in the Artic Ocean from 1958 to 1997, *J. Geophys. Res*., 105, 8789–8803, doi: 10.1029/1999JC900305.

Figure captions

Figure 1: Young Sound (YS) on the Greenland map. (b) The bathymetric map of YS following [*Rysgaard et al*., 2003]. Red crosses depict the CTD stations taken in May 2014. Yellow circles show the landfast ice-tethered oceanographic moorings deployed in October 2013. Black lines are the 100, 200 and 300 m depth contours. **(c-e)** SAR satellite imagery over the YS mouth. **(c)** 11/25/2013: Onset of the landfast ice. **(d)** 12/26/2013: Collapse of the landfast ice. The yellow-dashed rectangles contour the broken fast-ice floe blown downwind from the fast-ice edge during storm event in 12/18-12/25/2013 as indicated by white arrow. High radar backscatter strips appearing in gray/white indicate the new ice in the polynya area. **(e)** 01/29/2014: Coastal polynya. Low radar backscatter features appearing in black and gray indicate the coastal polynya open water with some fraction of new ice. The fast ice edge separates the landfast ice in YS and south of Clavering Ø from the coastal polynya. Yellow circles indicate mooring positions. The white-dashed rectangles p1-p3 contour the footprints of AMSR2 imagery. Yellow dashed

lines contour the coastal polynya regions 1-3 (highlighted with blue numbered arrows) used for the salt balance estimates.

Figure 2: Time series of **(a)** sea-ice concentration (%) from three AMSR2 pixels p1-p3 with footprints shown in Figure 1e - light yellow/green shading shows polynya/landfast ice over the YS mouth, **(b)** air temperature (°C, blue) and wind velocity (m/s, violet) at Daneborg meteorological station – orange shading indicates polynya wind events exceeding 15 m/s, **(c)** salinity and **(d)** temperature (solid lines, °C) and temperature of freezing (dotted lines, °C) computed for sea-surface using a standard algorithm by *Fofonoff and Millard* [1983] at 80 m (m02) and 77m (m03) from MMP and SBE-37, respectively, and **(e)** temperature (°C) at 2 m from the ADCP temperature sensor. **(b-e)** Blue, red and black lines show the 24-h running mean. Arrows on the bottom identify SAR images showing landfast ice (black), open water (dark blue) and new ice (blue) over the YS mouth.

Figure 3: The 24-h running mean of along-fjord current velocity (cm/s) at 6 m (dashed line) and 78 m (solid line) from the landfast ice-tethered ADCPs (positive/negative numbers correspond to the fjord inflow/outflow): **(a)** YS13-m02, **(b)** YS13-m03 and **(c)** YS13-04. Missing data are due to low acoustic backscatter. The shading is similar to that in Figure 2. The horizontal dashed and dotted lines in **(a-b)** show the along-fjord velocity derived from lagging the m02-m03 time series of temperature at 2 m (red) and salinity at 77-80 m (blue) – see text for more details. **(d)** The mean vertical profiles of along-fjord currents averaged for polynya period: YS13-m02 (black), YS13-m03 (blue) and YS13-m04 (red).

Figure 4: (a) Schematic depiction of polynya impact on the YS circulation. **(b)** Vertical distribution of temperature (red, °C), salinity (green) and DO (blue, ml/l) in 10/26/2013 (solid lines, temperature and salinity only) and 5/5/2014 (dashed lines) at mooring YS13-m04. **(c-d)** The along-fjord transect of **(c)** temperature (°C), **(d)** salinity and **(e)** DO (ml/l) taken in 5/10-12/2014 shows the polynya generated cool, saline and oxygen enriched water in ~40-140m. **(c)** Black triangles on the top identify positions of CTD stations. **(c-e)** Black and blue dashed lines show locations of the landfast ice-tethered moorings YS13-m03/m04 and landfast ice edge for 12/2013-03/2014, respectively.

Figure 5: Vertical distribution of **(a)** temperature (°C) and **(b)** salinity at stations 44 (red) and 40 (blue) located in ~3.5 km to the entrance sill at the sea- and lee-side of the sill, respectively. The sill depth is depicted with black dashed line. **(a)** For st. 44, the portion of the shelf water deeper than 60 m, modified due to interaction with Atlantic water, is highlighted with red dashed line. For station positions see Figure 1b.

Figures

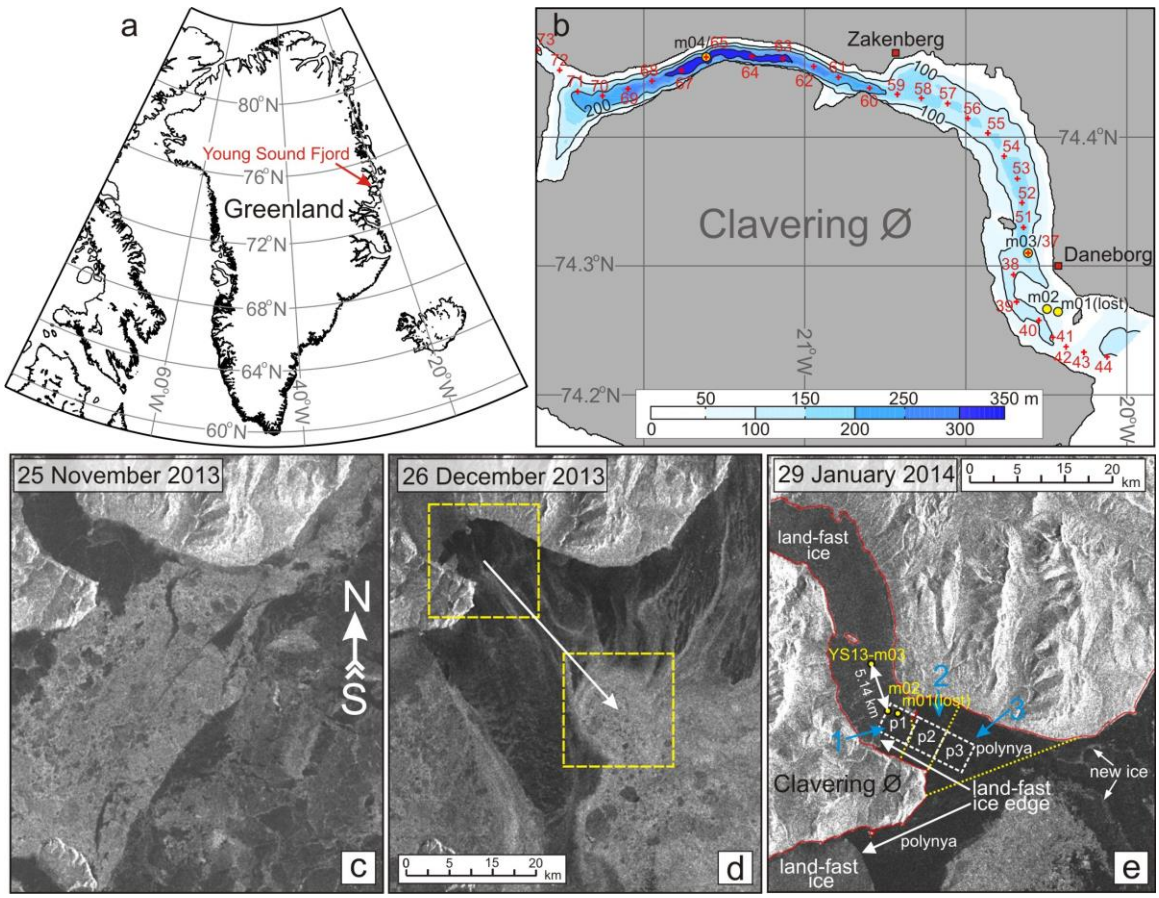

Figure 1: (a) Young Sound (YS) on the Greenland map. (b) The bathymetric map of YS following [*Rysgaard et al*., 2003]. Red crosses depict the CTD stations taken in May 2014. Yellow circles show the landfast ice-tethered oceanographic moorings deployed in October 2013. Black lines are the 100, 200 and 300 m depth contours. **(c-e)** SAR satellite imagery over the YS mouth. **(c)** 11/25/2013: Onset of the landfast ice. **(d)** 12/26/2013: Collapse of the landfast ice. The yellow-dashed rectangles contour the broken fast-ice floe blown downwind from the fast-ice edge during storm event in 12/18-12/25/2013 as indicated by white arrow. High radar backscatter strips appearing in gray/white indicate the new ice in the polynya area. **(e)** 01/29/2014: Coastal polynya. Low radar backscatter features appearing in black and gray indicate the coastal polynya open water with some fraction of new ice. The fast ice edge separates the landfast ice in YS and south of Clavering Ø from the coastal polynya. Yellow circles indicate mooring positions. The white-dashed rectangles p1-p3 contour the footprints of AMSR2 imagery. Yellow dashed lines contour the coastal polynya regions 1-3 (highlighted with blue numbered arrows) used for the salt balance estimates.

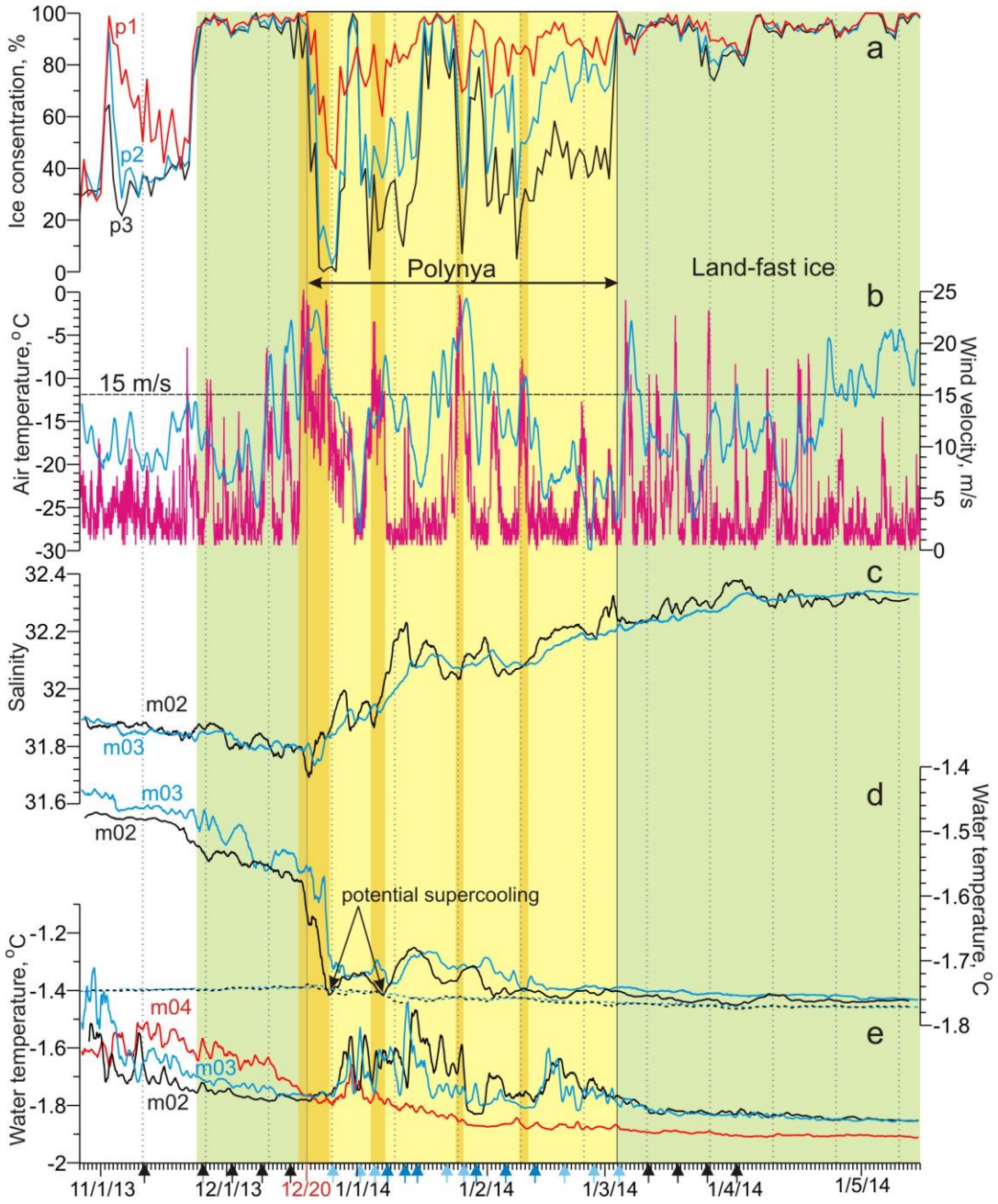

Figure 2: Time series of **(a)** sea-ice concentration (%) from three AMSR2 pixels p1-p3 with footprints shown in Figure 1e - light yellow/green shading shows polynya/landfast ice over the YS mouth, **(b)** air temperature (°C, blue) and wind velocity (m/s, violet) at Daneborg meteorological station – orange shading indicates polynya wind events exceeding 15 m/s, **(c)** salinity and **(d)** temperature (solid lines, °C) and temperature of freezing (dotted lines, °C) computed for sea-surface using a standard algorithm by *Fofonoff and Millard* [1983] at 80 m (m02) and 77m (m03) from MMP and SBE-37, respectively, and **(e)** temperature (°C) at 2 m from the ADCP temperature sensor. **(b-e)** Blue, red and black lines show the 24-h running mean. Arrows on the bottom identify SAR images showing landfast ice (black), open water (dark blue) and new ice (blue) over the YS mouth.

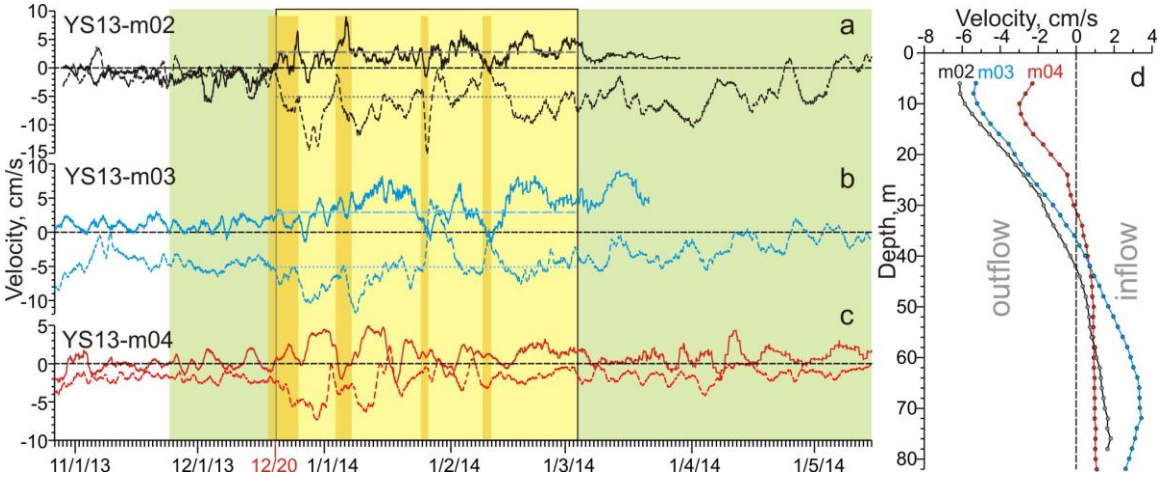

Figure 3: The 24-h running mean of along-fjord current velocity (cm/s) at 6 m (dashed line) and 78 m (solid line) from the landfast ice-tethered ADCPs (positive/negative numbers correspond to the fjord inflow/outflow): **(a)** YS13-m02, **(b)** YS13-m03 and **(c)** YS13-04. Missing data are due to low acoustic backscatter. The shading is similar to that in Figure 2. The horizontal dashed and dotted lines in **(a-b)** show the along-fjord velocity derived from lagging the m02-m03 time series of temperature at 2 m (red) and salinity at 77-80 m (blue) – see text for more details. **(d)** The mean vertical profiles of along-fjord currents averaged for polynya period: YS13-m02 (black), YS13-m03 (blue) and YS13-m04 (red).

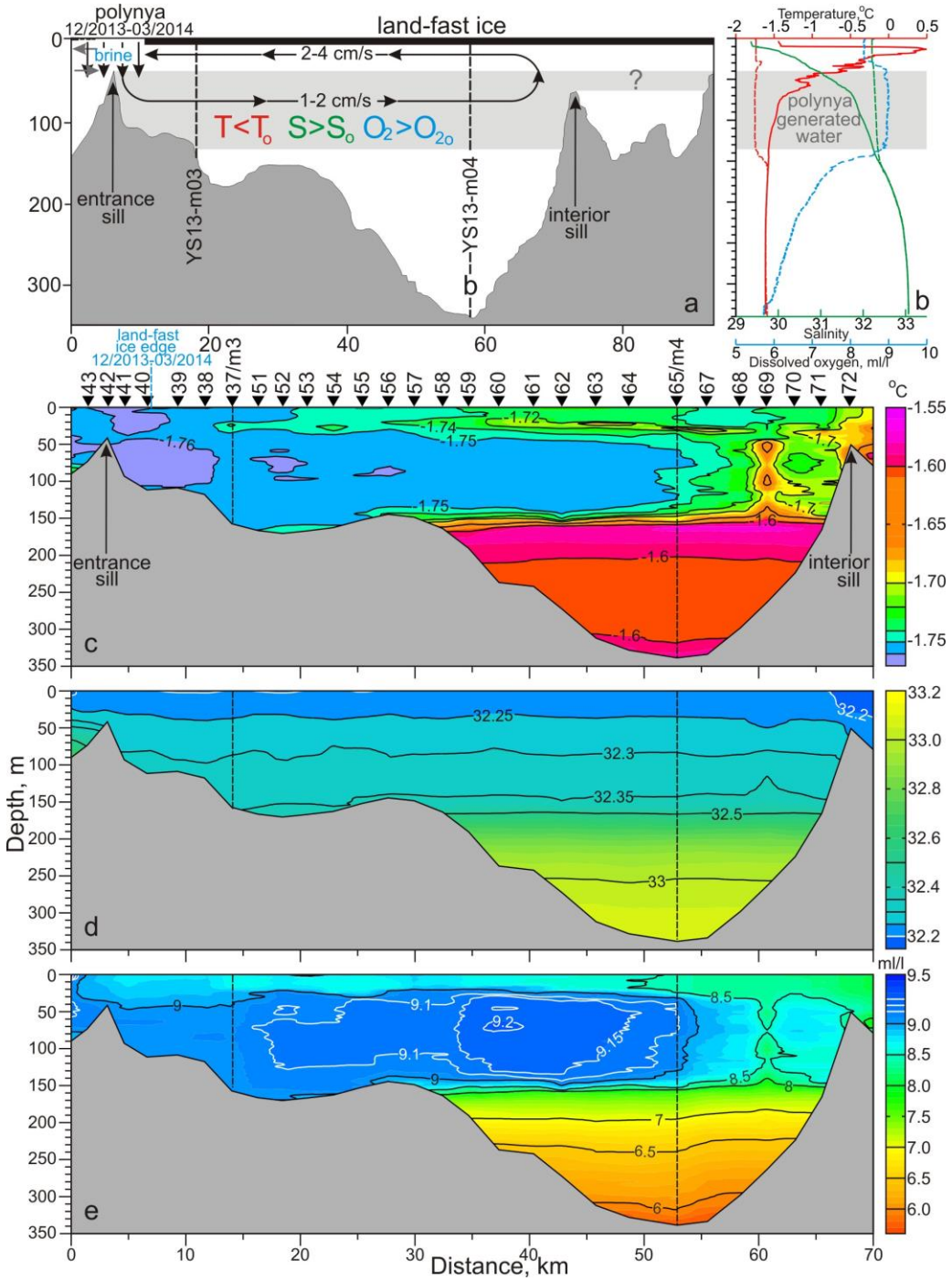

Figure 4: (a) Schematic depiction of polynya impact on the YS circulation. **(b)** Vertical distribution of temperature (red, °C), salinity (green) and DO (blue, ml/l) in 10/26/2013 (solid lines, temperature and salinity only) and 5/5/2014 (dashed lines) at mooring YS13-m04. **(c-d)** The along-fjord transect of **(c)** temperature (°C), **(d)** salinity and **(e)** DO (ml/l) taken in 5/10-12/2014 shows the polynya generated cool, saline and oxygen enriched water in ~40-140 m. **(c)** Black triangles on the top identify positions of CTD stations. **(c-e)** Black and blue dashed lines show locations of the landfast ice-tethered moorings YS13-m03/m04 and landfast ice edge for 12/2013-03/2014, respectively.

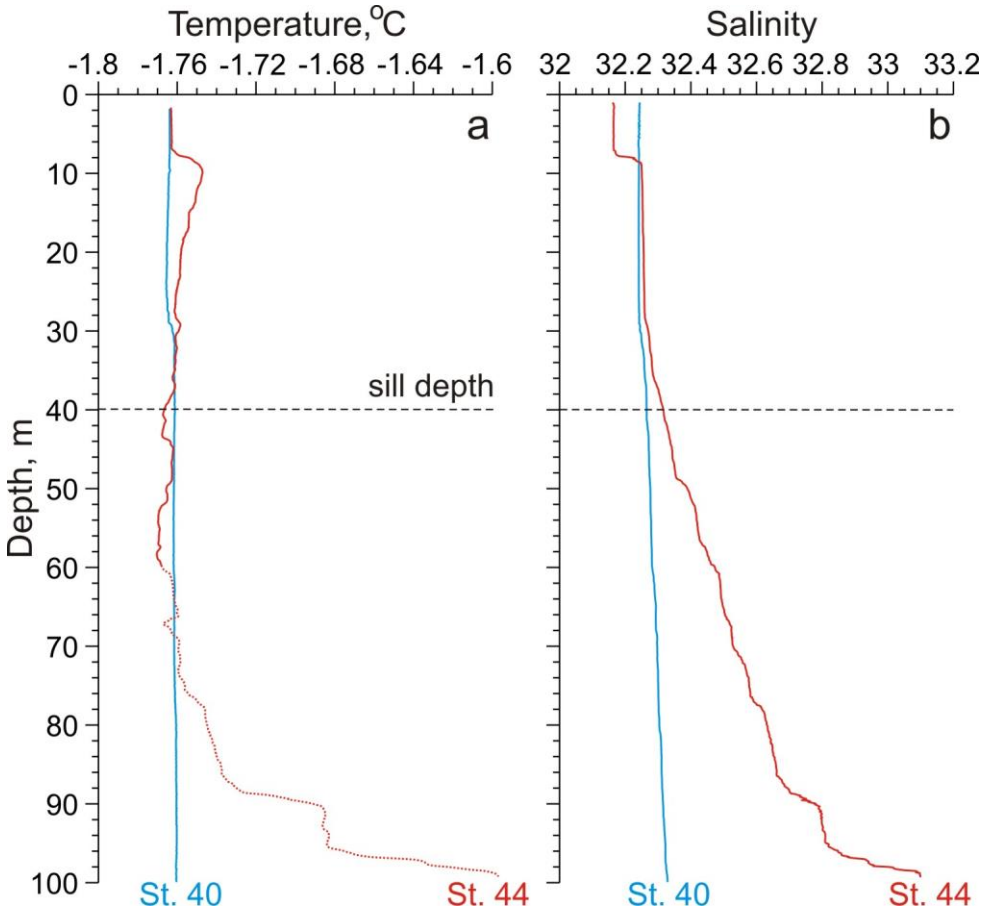

Figure 5: Vertical distribution of **(a)** temperature (°C) and **(b)** salinity at stations 44 (red) and 40 (blue) located in ~3.5 km to the entrance sill at the sea- and lee-side of the sill, respectively. The sill depth is depicted with black dashed line. (a) For st. 44, the portion of the shelf water deeper than 60 m, modified due to interaction with Atlantic water, is highlighted with red dashed line. For station positions see Figure 1b.